national accelerator laboratory

NAL-Conf-74/68-EXP

# RECENT FERMILAB BUBBLE CHAMBER EXPERIMENTS AND RESULTS

L. Voyvodic

July 1974

(Paper presented at the Vth International Conference
on Multiparticle Hadrodynamics, Leipzig, June 2-10, 1974)

# RECENT FERMILAB BUBBLE CHAMBER EXPERIMENTS AND RESULTS

L. Voyvodic
Fermi National Accelerator Laboratory
Batavia, Illinois 60510

## ABSTRACT

An over-view is given of experiments using the 30-inch hydrogen bubble chamber during the past two years. Emphasis is given to increased capabilities provided by beam tagging and hybrid spectrometer systems in the more recent experiments. Summary results are discussed for pp and $\pi$p collisions at high energies, in multiplicity distributions, in exclusive and inclusive reaction studies.

## SUMMARY OF EXPERIMENTS

A summary of experiments carried out with the 30-inch hydrogen bubble chamber at FermiLab is shown in Figure 1. It can be seen from the scale that approximately 0.2 million pictures were taken during the first year of operation, and about 1.0 million additional pictures during the second year just ended.

Much of this increase in picture-taking has been due to improvements in accelerator operation and ability to send typically four beam spills to the bubble chamber during each acceleration cycle.

The physics results available to date chiefly come from the pp and $\pi^- p$ exposures taken in the first year. The newer experiments, which are also more complex, are still largely in the analysis stage. The complexity and enhanced scope of the latter arise from the following additional experimental features:

1) A beam tagging system which provides computer logging of each beam particle seen in the bubble chamber. The record includes particle position, direction and momentum as it enters the fiducial volume, as derived from a set of upstream proportional wire chambers. Particle mass information comes from a differential Cerenkov counter. The

record also shows whether the beam particle had triggered downstream spectrometer logic, or penetrated a thick muon-identifying absorber beyond the spectrometer.

2) Methods have been introduced[1] for enriching the fraction of wanted particles. For example, the 200 GeV $\pi^+ p$ exposure in Figure 1 utilized a secondary particle filter to enhance the $\pi^+$ (and $K^+$) content at the bubble chamber, by preferential absorption of the secondary proton component. Other methods, including decay products and re-targetting of secondary particles, are being studies for $\bar{p}$ and $\bar{K}$ enrichments for future experiments with both the 30-inch and 15-foot bubble chambers.

3) Hybrid chamber spectrometer systems provide further analysis of secondary particles emerging downstream of the bubble chamber. The 150 GeV $\pi^- p$ exposure in Figure 1 utilized a set of proportional wire chambers[2] for this purpose, while the majority of the hybrid system exposures in Figure 1 were taken with large wide-gap spark chambers[3]. Both systems utilize the bubble chamber fringe field and relatively long lever

arms to gain additional momentum and directional accuracy. Lead converters are also used between the farthest downstream chambers for detecting forward-going gamma rays.

## RECENT BARE CHAMBER RESULTS

Topological cross-sections $\sigma_n$ and mean multiplicities $\langle n \rangle$ from high energy bubble chamber experiments have been reviewed recently by Berger et al[4]. Figure 2 shows part of their compilation, bringing out the following features:

(a) The weighted prong distribution follows closely the type of scaling predicted by Koba, Nielsen and Oleson,

(b) Multiplicity distributions are very similar for proton and pion projectiles, and

(c) Some significant differences may exist at low multiplicities (large values of $\langle n \rangle/n$ in their representation) and are useful clues to dynamical effects such as diffractive processes.

Results from the simplest type of event analysis; i.e., recoil proton measurements, have been compared by Winkelman[5] for data from the two 205 GeV experiments on $pp \to p+x$ and $\pi^- p \to p+x$. Close similarities are found for diffractive enhancements in 2, 4 and 6 prong multiplici-

ties at low missing mass, as well as similarities in the inclusive missing mass ($M^2$) distributions.

Studies made of the important four body reactions $pp \to pp\ \pi^+\ \pi^-$ and $\pi^- p \to \pi^- p\ \pi^+\ \pi^-$ have been reviewed by Whitmore[6]. Figure 3 shows his energy dependence of the cross-section for this exclusive channel. A notable feature is that the 200 GeV results from early experiments in Figure 1 appear to be nearly twice as large as expected from extrapolations at low energies. About 60% of the four-prong events with recoil proton are represented in this exclusive channel[5]. In view of the increased statistics and precision expected in the newer FermiLab experiments, special interest will be attached to overcoming present limitation[6] on double Pomeron tests and other mechanisms in these channels.

Inclusive charged and neutral particle distributions, and multiparticle correlations data have also been reviewed by Whitmore[6] for the earlier experiments in Figure 1.

## RECENT HYBRID SYSTEM RESULTS

Momentum accuracy of the 30-inch chamber alone is shown in Figure 4 to be poorer than 10% for secondary particles above 15 GeV/c (which means that chiefly the particles in the backward hemisphere are measurable for bombarding energies above about 100 GeV). Also shown in Figure 4

is the dramatic improvement in accuracy provided by hooking up the tracks in the wide-gap spark chambers back to the bubble chamber vertex[3]. In this case even leading particles with momenta near 200 GeV/c can be measured with errors under 10%.

Examples of hybrid system momentum results are shown in Figure 5, from Shephard et al[7]. The $\pi^-$ production of interest here is dominantly in the forward hemisphere and at high laboratory momenta. Thus, the accuracy of the hybrid system allows reliable determination of momentum P, of transverse momentum ($P_t$) and of rapidity (y). Two features which stand out in Figure 5 are (1) the approach to scaling in $P_t^2$ from below, and (2) indication of factorization at the lower vertex (negative values of rapidity y) in $\pi^-p$ and pp production of $\pi^-$. There are some questions whether these latter features also hold semi-inclusively. Questions of this kind, as well as kinematic tests are being studied in current systematic analyses for each topology in the various hybrid experiments.

Gamma-ray detection in the forward $\pm 4^0$ cone is provided by lead plates in front of the fourth spark chamber. After taking into account the acceptance geometry, exit wall attenuation, radiator thickness and uncertainties in recognizing low energy photons, prelim-

inary results[8] are shown in Figure 6 for the normalized number of gamma-rays produced per inelastic 200 GeV pp collision. The multiplicity distribution in Figure 6 leads to the following values for the mean $\pi^o$ multiplicity $\langle n_{\pi^o} \rangle$ and $\pi^o$-$\pi^o$ correlation parameter $f_{2^{oo}}$:

$$\langle n_{\pi^o} \rangle = 3.4 \pm 0.1; \quad f_{2^{oo}} = -0.5 \pm 0.6$$

More complete results and definitive comparisons with theories are expected from the analyses in progress on interactions at 300 GeV and higher, where the solid angle acceptance allows fuller detection of $\pi^o$ and gamma-rays from the central region and backward hemisphere.

---

REFERENCES

(1) W.W.Neale, FermiLab report FN-259 (1974)

(2) W.Bugg et al., Bulletin APS 19, 96 (1974)

(3) G.A.Smith, "Particles and Fields 1973", AIP Conference Proceedings, Berkeley, p. 500 (1973)

(4) E.L.Berger et al., CERN preprint D.PH.II/Phys. 74-9 (1974)

(5) F.C.Winkelmann, Physics Letters 48B, 273 (1974)

(6) J.Whitmore, Physics Reports 1974 (in press)

(7) W.D.Shephard et al., submitted to XVII Int. Conf. on High Energy Physics, London, July 1974

(8) G.A.Smith and collaboration, submitted to XVII Int. Conf. on High Energy Physics, London, July 1974

FIGURE CAPTIONS

Figure 1 Summary of 30-inch hydrogen bubble chamber experiments.

Figure 2 Charged multiplicity cross-sections "scaling" plot for a) $\pi^- p$ interactions and b) pp interactions at high energies.

Figure 3 The cross-sections for the ractions (a) $pp \rightarrow pp\pi^+\pi^-$ and (b) $\pi^- p \rightarrow \pi^- p\pi^+\pi^-$ as a function of the incident momentum. The solid lines are the results of fits to the form $\sigma = ap_{lab}^{-n}$ and the dashed lines are the same forms extrapolated to ~200 GeV/c

Figure 4 Scatter plot of momentum accuracy $\Delta p/p$ versus p for secondary tracks from 15 to 200 GeV/c based on (a) bubble chamber along (open circles) and (b) hybrid system (closed circles).

Figure 5 Inclusive distributions for $\pi^-$ production, in transverse momentum $P_t$ from 205 and 18.5 GeV/c $\pi^- p$ interactions, and in rapidity y from 205 GeV/c $\pi^- p$ and pp interactions

Figure 6 The normalized distribution of gamma-rays, $N_\gamma$ observed in 200 GeV pp inelastic collisions, after removing showers with three or fewer electrons.

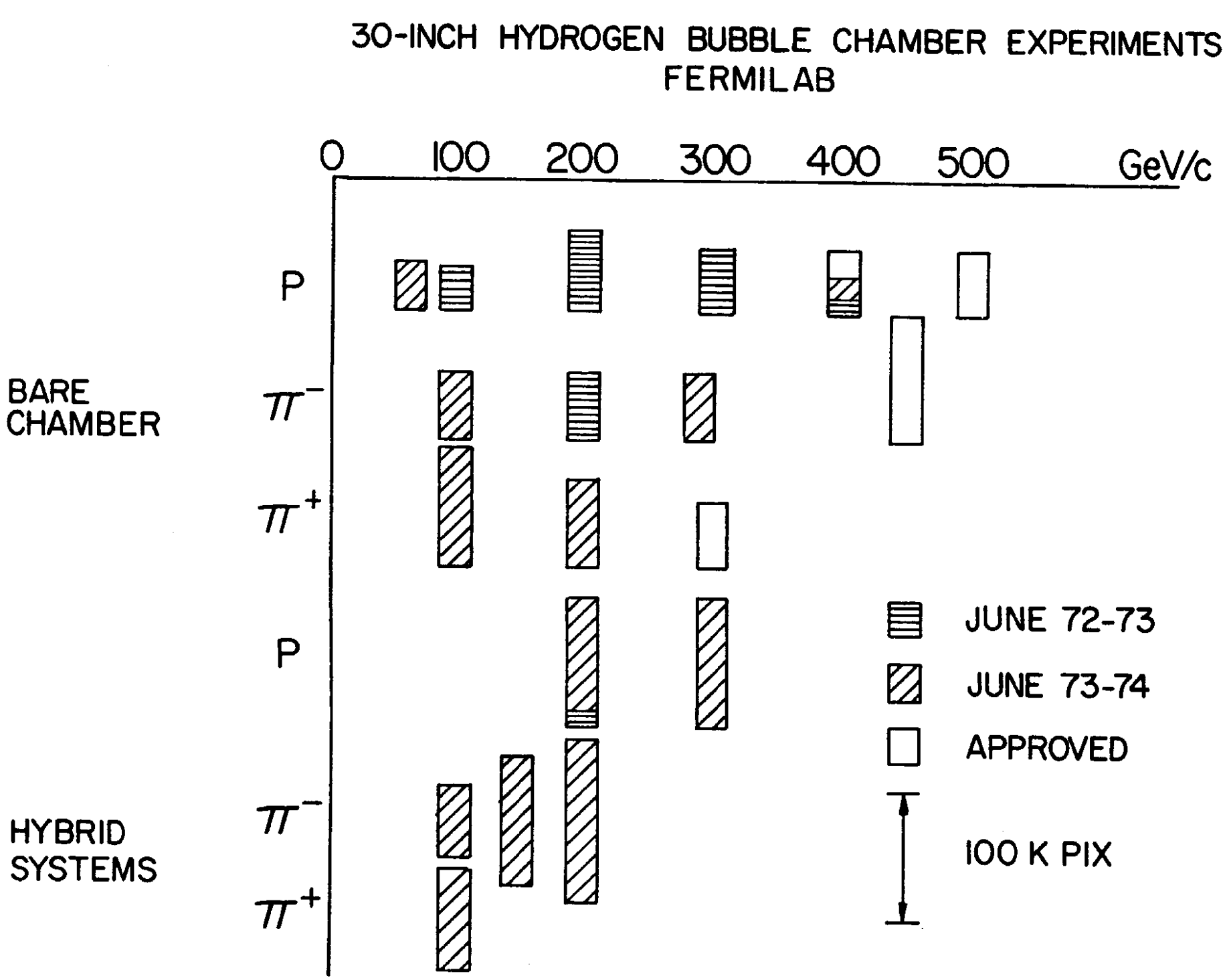
30-INCH HYDROGEN BUBBLE CHAMBER EXPERIMENTS
FERMILAB
0
100
200
300
400
500
GeV/c
BARE CHAMBER
HYBRID SYSTEMS
P
$\pi^-$
$\pi^+$
P
$\pi^-$
$\pi^+$
JUNE 72-73
JUNE 73-74
APPROVED
100 K PIX

FIGURE 1

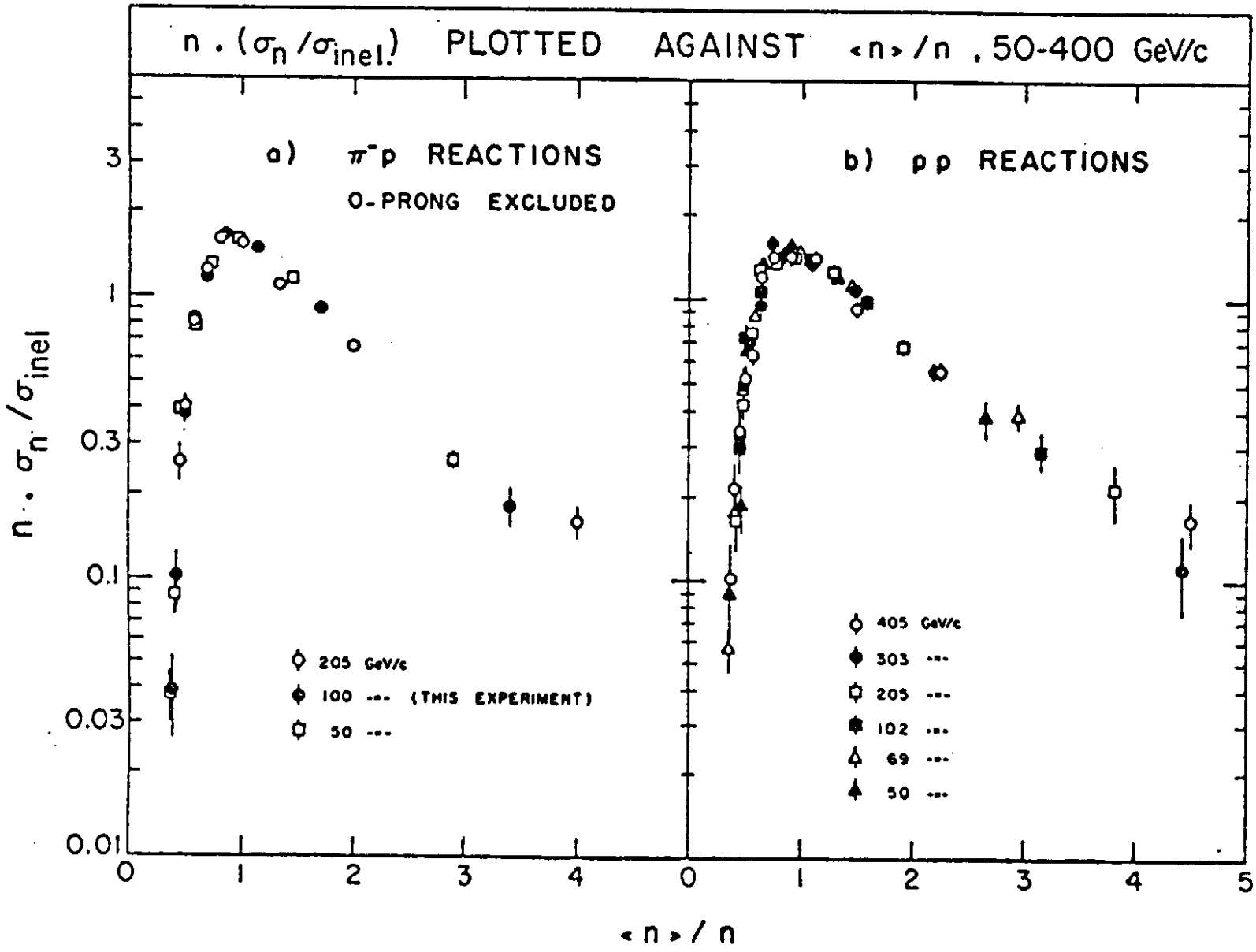
n . (σn /σinel.) PLOTTED AGAINST <n> / n , 50-400 GeV/c
a) π⁻p REACTIONS
0-PRONG EXCLUDED
205 GeV/c
100 --- (THIS EXPERIMENT)
50 ---
b) p p REACTIONS
405 GeV/c
303 ---
205 ---
102 ---
69 ---
50 ---
n . σn /σinel
<n> / n
0.01
0.03
0.1
0.3
1
3
0
1
2
3
4
5

FIGURE 2

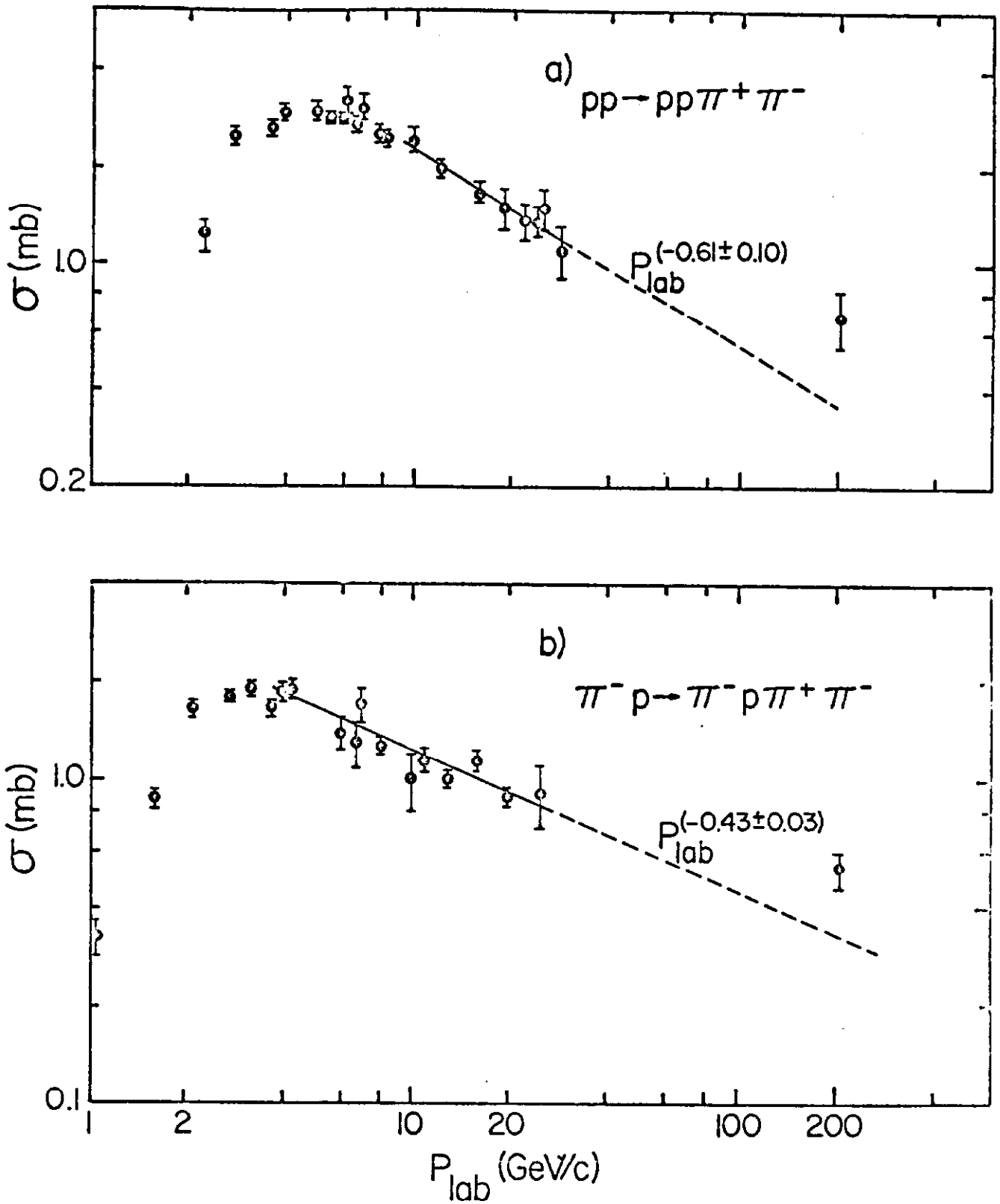
a)
pp → pp π+ π−
σ (mb)
1.0
0.2
P lab (−0.61 ± 0.10)
b)
π− p → π− p π+ π−
σ (mb)
1.0
0.1
P lab (−0.43 ± 0.03)
1
2
10
20
100
200
P lab (GeV/c)

FIGURE 3

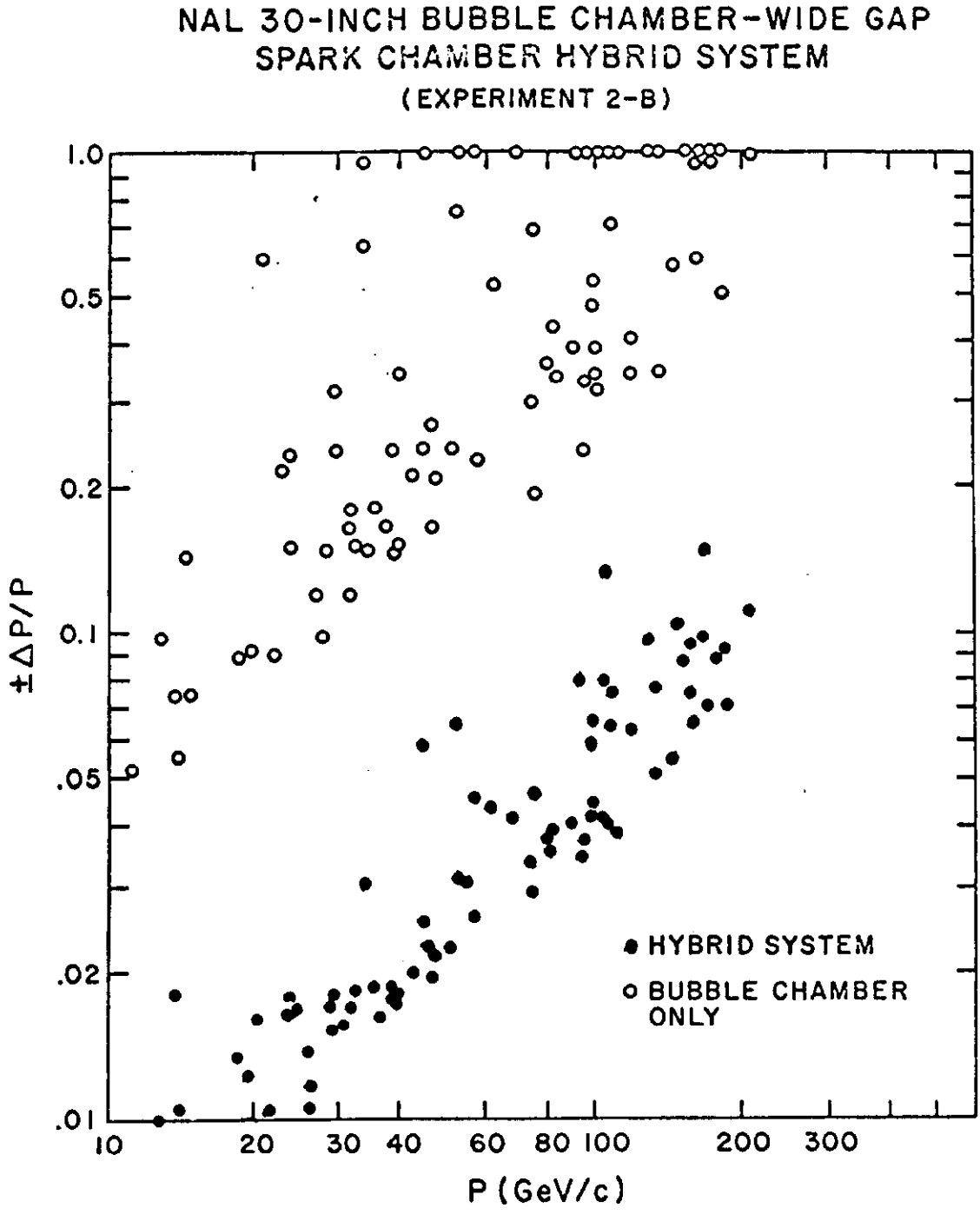
NAL 30-INCH BUBBLE CHAMBER-WIDE GAP
SPARK CHAMBER HYBRID SYSTEM
(EXPERIMENT 2-B)
1.0
0.5
0.2
0.1
.05
.02
.01
±ΔP/P
10
20
30
40
60
80
100
200
300
P (GeV/c)
HYBRID SYSTEM
BUBBLE CHAMBER ONLY

FIGURE 4

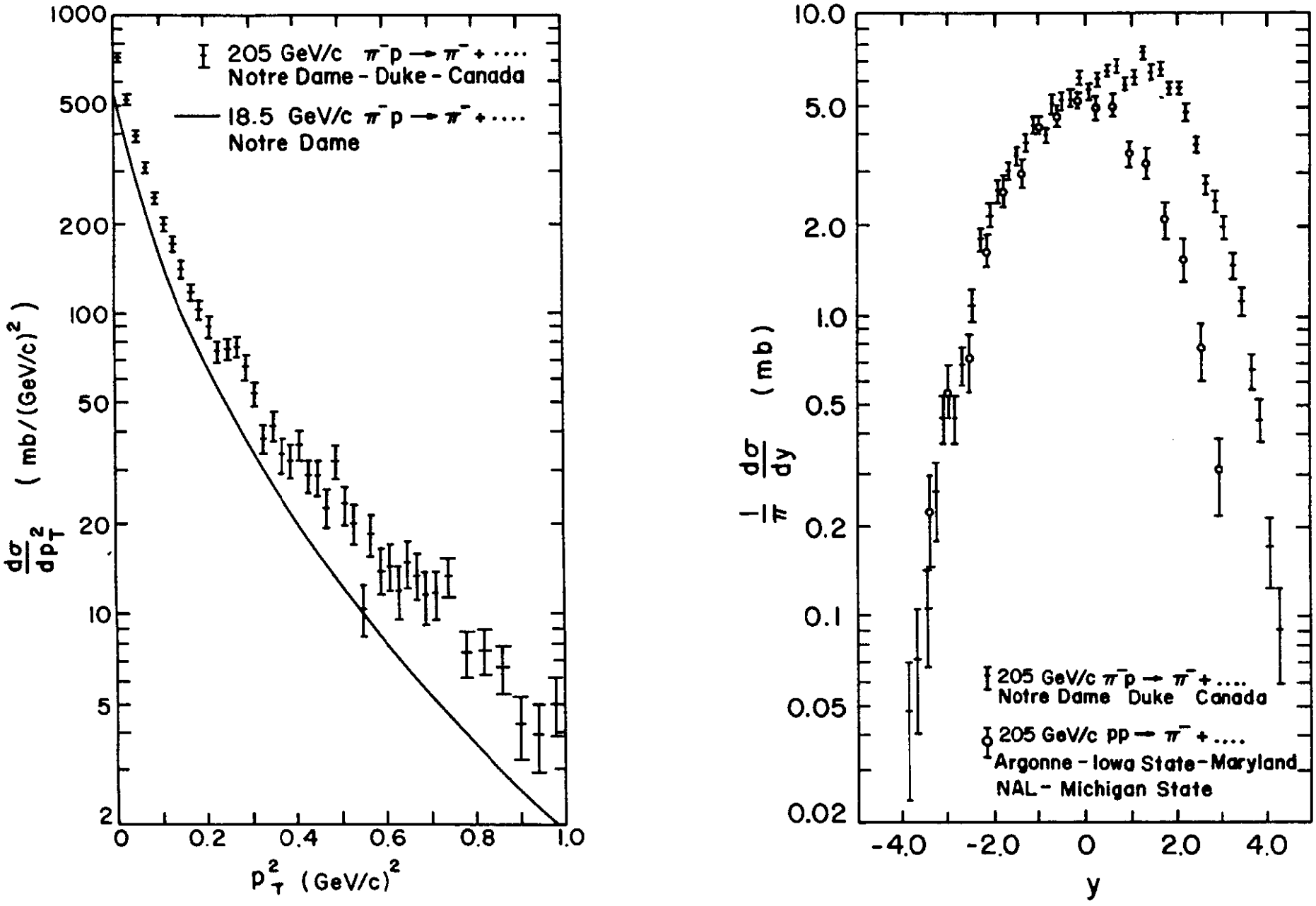
205 GeV/c π⁻p → π⁻ + ····
Notre Dame - Duke - Canada
18.5 GeV/c π⁻p → π⁻ + ····
Notre Dame
dσ/dp_T² ( mb/(GeV/c)² )
p_T² (GeV/c)²
1000
500
200
100
50
20
10
5
2
0
0.2
0.4
0.6
0.8
1.0
-1/π dσ/dy (mb)
y
10.0
5.0
2.0
1.0
0.5
0.2
0.1
0.05
0.02
-4.0
-2.0
0
2.0
4.0
205 GeV/c π⁻p → π⁻ + ····
Notre Dame Duke Canada
205 GeV/c pp → π⁻ + ····
Argonne - Iowa State - Maryland
NAL - Michigan State

FIGURE 5

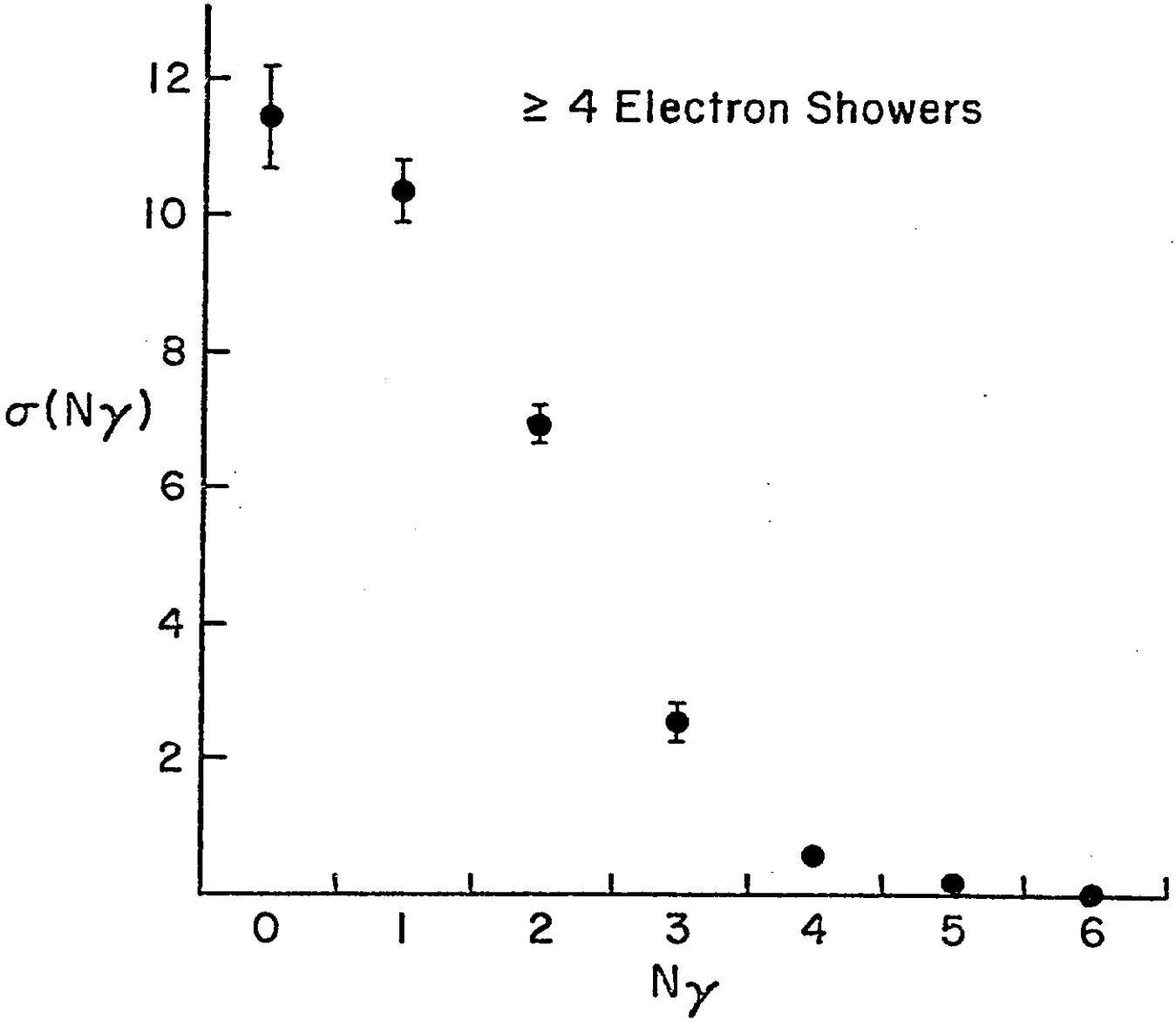


FIGURE 6